Available online at www.sciencedirect.com
ScienceDirect
*Chinese Journal of Natural Medicines* 2022, **20**(2): 155-160
doi: 10.1016/S1875-5364(21)60103-6
Chinese Journal of Natural Medicines

•Research article•

# Three new ursane-type triterpenoids from *Rosmarinus officinalis* and their biological activities

ZHONG Xiang-Jian[1Δ], ZHOU Na[1Δ], WANG Xin[1], LI Jin-Jie[1], MA Hui[2], JIAO Yue[1], XU Jia-Hui[1], LIN Peng-Cheng[3], SHANG Xiao-Ya[1*]

[1] *Beijing Key Laboratory of Bioactive Substances and Functional Foods, Beijing Union University, Beijing 100191, China;*
[2] *Shandong Institute for Product Quality Inspection, Jinan 250100, China;*
[3] *Key Laboratory for Qinghai-Tibet Plateau Phytochemistry of Qinghai Province, Qinghai Nationalities University, Xining 810000, China*

Available online 20 Feb., 2022

**[ABSTRACT]** Three new ursane-type triterpenoids, 3-oxours-12-en-20, 28-olide (**1**), 3*β*-hydroxyurs-12-en-20, 28-olide (**2**) and 3*β*-hydroxyurs-11, 13(18)-dien-20, 28-olide (**3**), were isolated from a potent anti-inflammatory and antibacterial fraction of the ethanolic extract of *Rosmarinus officinalis*. Their structures were elucidated by a combination of extensive 1D- and 2D-NMR experiments, MS data and comparisons with literature reports. Compounds **1**−**3** exhibited significantly inhibitory effects on nitric oxide production in lipopolysaccharide-activated mouse RAW264.7 macrophages, but no antibacterial activity was found at a concentration of 128 μg·mL$^{-1}$.

**[KEY WORDS]** *Rosmarinus officinalis*; Isolation and purification; Triterpenoid; Biological activity
**[CLC Number]** R284.1 **[Document code]** A **[Article ID]** 2095-6975(2022)02-0155-06

## Introduction

*Rosmarinus officinalis*, originating from the Mediterranean basin, belongs to the Lamiaceae family. It is a woody and perennial herb with a strong pleasant odor, which is commonly named rosemary. Rosemary is one of the most widely commercialized culinary herbs and has been used as a food seasoning as well as an antioxidant in processed foods and cosmetics [1]. Rosemary is also a medicinal plant and its extracts or components have strong anti-inflammatory, antioxidant, antibacterial, antifungal, antidiabetic and hepatoprotective activities [2]. Some studies have reported that the anti-inflammatory and antibacterial activities of rosemary extract are closely related to its compounds such as carnosic acid, carnosol and ursolic acid [3-8]. However, Elena Arranz *et al*. found that the anti-inflammatory activity of carnosic acid and rosmarinic acid was weaker than that of the crude extract in rosemary [9-10]. Furthermore, some studies suggested that the antibacterial activity was related not only to the major components but also to the minor components in the oil [11-12]. To date, the major components in rosemary that contribute to its anti-inflammatory and antibacterial activities remain unclear.

In the current study, carnosic acid, carnosol and ursolic acid were removed from rosemary extracts by chromatographic methods, but the remaining fraction still exhibited potent anti-inflammatory and antibacterial activities. In the remaining fraction, three new ursane-type triterpenoids were isolated, and their structures were elucidated by NMR experiments and mass spectrometry. Furthermore, their anti-inflammatory and antibacterial activities were evaluated *in vitro*. The results confirmed that the three new compounds displayed significantly inhibitory effects on nitric oxide (NO) production in lipopolysaccharide (LPS)-activated mouse RAW264.7 macrophages.

## Results and Discussion

### *Chemical structure elucidation*

Compound **1** was purified as white amorphous powder.

**[Received on]** 17-May-2021
**[Research funding]** This work was supported by the Key Projects of Beijing Natural Sciences Foundation and Beijing Municipal Education Committee (No. KZ201811417049), the Scientific Research Common Program of Beijing Municipal Commission of Education (No. KM202011417014), the Innovation Platform for the Development and Construction of Special Project of Key Laboratory for Tibet Plateau Phytochemistry of Qinghai Province (No. 2019-ZJ-Y19), Beijing Union University Graduate Research and Innovation Fund Project (No. YZ2020K001) and the Academic Research Projects of Beijing Union University (No. XP202005).
[*]**Corresponding author]** E-mail: shangxiaoya@buu.edu.cn
[Δ]These authors contributed equally to this work.
These authors have no conflict of interest to declare.

Its molecular formula $C_{30}H_{44}O_3$, requiring nine degrees of unsaturation, was deduced from HR-ESI-MS at *m/z* 453.3362 $[M + H]^+$ (Calcd. for $C_{30}H_{45}O_3$, 453.3363) combined with the NMR data (Table 1). The MS/MS spectrum gave fragment ions at *m/z* 435.3255, 407.3306, 389.3200, 201.1636, and 189.1637. Its IR spectrum suggested that it contained carbonyl groups (1739 and 1704 $cm^{-1}$). The $^1H$ NMR spectrum of **1** displayed six singlets of methyl groups ($\delta_H$ 0.70, 0.94, 1.03, 1.05, 1.17 and 1.25), a doublet of methyl group [$\delta_H$ 0.96 (3H, d, *J* = 7.0 Hz)], and an olefinic resonance at $\delta_H$ 5.40

**Table 1 $^1H$ NMR and $^{13}C$ NMR data for compounds 1–3 (*J* in Hz)**

| No. | 1 | | 2 | | 3 | |
|---|---|---|---|---|---|---|
| | $\delta_H$ (mult, *J*) | $\delta_C$ (mult) | $\delta_H$ (mult, *J*) | $\delta_C$ (mult) | $\delta_H$ (mult, *J*) | $\delta_C$ (mult) |
| 1 | (a) 1.27 (1H, m)<br>(b) 1.65 (1H, m) | 38.4 | (a) 1.03 (1H, m)<br>(b) 1.58 (1H, m) | 38.1 | (a) 1.06 (1H, m)<br>(b) 1.88 (1H, m) | 38.2 |
| 2 | (a) 2.39 (1H, ddd, 12.5, 7.0, 6.5)<br>(b) 2.60 (1H, ddd, 17.3, 7.0, 6.5) | 34.2 | 1.63 (2H, m) | 27.2 | 1.70 (2H, m) | 27.2 |
| 3 | | 215.9 | 3.23 (1H, dd, 11.0, 5.0) | 79.2 | 3.24 (1H, dd, 11.5, 5.0) | 79.1 |
| 4 | | 47.5 | | 38.9 | | 39.0 |
| 5 | 1.31 (1H, m) | 55.4 | 0.80 (1H, m) | 55.7 | 0.79 (1H, m) | 54.9 |
| 6 | 1.43 (2H, m) | 19.9 | (a) 1.44 (1H, m)<br>(b) 1.59 (1H, m) | 18.7 | (a) 1.41 (1H, m)<br>(b) 1.60 (1H, m) | 18.3 |
| 7 | 1.21 (2H, m) | 32.1 | 1.34 (2H, m) | 32.7 | 1.36 (2H, m) | 32.7 |
| 8 | | 39.4 | | 39.6 | | 41.4 |
| 9 | 1.79 (1H, m) | 47.6 | 1.79 (1H, m) | 48.3 | 1.98 (1H, m) | 54.3 |
| 10 | | 37.4 | | 38.0 | | 36.9 |
| 11 | (a) 1.00 (1H, m)<br>(b) 1.88 (1H, m) | 24.0 | (a) 1.87 (1H, m)<br>(b) 2.11 (1H, m) | 24.2 | 6.10 (1H, dd, 10.3, 3.2) | 126.1 |
| 12 | 5.40 (1H, br s) | 121.2 | 5.40 (1H, t, 2.8) | 121.4 | 5.73 (1H, dd, 10.3, 2.0) | 128.1 |
| 13 | | 140.5 | | 140.6 | | 137.4 |
| 14 | | 41.9 | | 41.9 | | 41.5 |
| 15 | (a) 1.62 (1H, m)<br>(b) 2.11 (1H, m) | 23.4 | (a) 1.10 (1H, ddd, 13.8, 5.7, 1.9)<br>(b) 1.63 (1H, m) | 23.3* | (a) 1.16 (1H, dt, 13.2, 3.5)<br>(b) 1.55 (1H, m) | 25.6 |
| 16 | (a) 1.36 (1H, m)<br>(b) 3.22 (1H, dd, 5.8, 14.8) | 23.7 | (a) 1.31 (1H, m)<br>(b) 2.91 (1H, ddd, 15.0, 6.1, 1.9) | 23.4* | (a) 1.36 (1H, m)<br>(b) 2.52 (1H, ddd, 14.1, 4.2, 2.8) | 25.3 |
| 17 | | 39.4 | | 39.3 | | 42.6 |
| 18 | 1.90 (1H, m) | 48.6 | 1.80 (1H, m) | 48.6 | | 134.4 |
| 19 | 1.83 (1H, m) | 37.8 | 1.83 (1H, m) | 37.7 | 2.67 (1H, q, 7.0) | 40.8 |
| 20 | | 81.5 | | 82.0 | | 83.0 |
| 21 | (a) 1.57 (1H, m)<br>(b) 1.65 (1H, m) | 34.9 | (b) 1.64 (1H, m)<br>(a) 1.76 (1H, m) | 35.0 | (a) 1.76 (1H, m)<br>(b) 1.92 (1H, m) | 32.9 |
| 22 | (a) 1.43 (1H, m)<br>(b) 2.02 (1H, ddd, 15.5, 7.0, 5.0) | 28.7 | (a) 1.50 (1H, m)<br>(b) 2.08 (1H, m) | 28.6 | (a) 1.61 (1H, m)<br>(b) 1.96 (1H, m) | 34.0 |
| 23 | 1.17 (3H, s) | 26.3 | 0.99 (3H, s) | 28.2 | 0.99 (3H, s) | 28.0 |
| 24 | 1.05 (3H, s) | 21.3 | 0.79 (3H, s) | 15.5 | 0.78 (3H, s) | 15.2 |
| 25 | 0.94 (3H, s) | 14.7 | 0.89 (3H, s) | 15.6 | 0.90 (3H, s) | 18.3* |
| 26 | 0.70 (3H, s) | 15.8 | 0.72 (3H, s) | 16.1 | 0.70 (3H, s) | 16.1 |
| 27 | 1.03 (3H, s) | 21.3 | 1.05 (3H, s) | 21.5 | 0.94 (3H, s) | 18.4* |
| 28 | | 178.4 | | 179.3 | | 176.2 |
| 29 | 0.96 (3H, d, 7.0) | 17.3 | 1.03 (3H, d, 6.5) | 17.5 | 1.08 (3H, d, 7.0) | 16.4 |
| 30 | 1.25 (3H, s) | 22.5 | 1.31 (3H, s) | 22.7 | 1.40 (3H, s) | 23.0 |

$^1H$ and $^{13}C$ NMR data were measured in $C_5D_5N$ for **1** and $CDCl_3$ for **2**–**3** at 500 and 125 MHz. The assignments were based on DEPT, $^1H$-$^1H$ COSY, HSQC and HMBC experiments. *Data are interchangeable.

(br s). The $^{13}$C NMR spectrum associated with DEPT and HSQC spectra of **1** showed 30 carbon signals, which were seven methyls, nine methylenes, five methines, and nine quaternary carbons, including one oxygen-bearing carbon at $\delta_C$ 81.5, two olefinic carbons at $\delta_C$ 121.2 and $\delta_C$ 140.5, one ester carbonyl carbon at $\delta_C$ 178.4 and one ketocarbonyl carbon at $\delta_C$ 215.9. The above NMR spectroscopic data indicated that **1** was similar to the known ursane-type triterpenoid, *α*-amyrenone [13-14], except for an additional six-membered lactone ring that satisfied the nine degrees of unsaturation represented by the molecular formula. In the HMBC spectrum, the long-range correlations from H-18 ($\delta_H$ 1.90) to C-12, C-13, C-16, C-19, C-22, C-28 and C-29, from $H_3$-30 ($\delta_H$ 1.25) to C-28, C-20, C-21 and C-19, and from H-16b ($\delta_H$ 3.22) to C-14, C-15, C-17, C-18, C-22 and C-28 suggested the presence of a six-membered lactone ring between C-20 and C-28. Accordingly, the planar structure of **1** was determined (Fig. 1).

The relative stereochemistry of **1** was elucidated by analysis of the NOESY spectrum, and the correlations between Me-23/H-5, H-5/H-9, H-9/Me-27, Me-27/H-18, Me-29/H-18 and Me-30 revealed that these protons were cofacial with an *α*-configuration, whereas the correlations between Me-25/Me-24 and Me-26 corresponded to be on the other side of the molecular plane with a *β*-orientation (Fig. 2). Based on the above spectral evidence, the structure of **1** was unambiguously established as 3-oxours-12-en-20,28-olide.

Compound **2** was obtained as white amorphous powder. The HR-ESI-MS at *m/z* 455.3519 $[M + H]^+$ (Calcd. for $C_{30}H_{47}O_3$, 455.3520), for the formula of $C_{30}H_{46}O_3$, indicated eight degrees of unsaturation, which was consistent with the NMR data (Table 1). The MS/MS spectrum gave fragment ions at *m/z* 437.3417, 409.3467, 391.3357, 201.1638, and 187.1481. In the IR spectrum of **2**, the absorptions at 3509 $cm^{-1}$ and 1730 $cm^{-1}$ suggested the presence of hydroxyl and carbonyl groups respectively. According to the 1D NMR spectra, the chemical structure of **2** was very similar to compound **1**, except that the C-3 carbonyl carbon at $\delta_C$ 215.9 was replaced by an oxygen-bearing carbon at $\delta_C$ 79.2, and the proton signal of H-3 appeared at $\delta_H$ 3.23 in 1D NMR data (Table 1). The relative configuration of **2** was deduced by the coupling constants and NOESY spectrum. The coupling constants of H-3 at $\delta_H$ 3.23 (dd, $J$ = 11.0, 5.0 Hz) confirmed that the 3-hydroxy group was *β*-oriented. In the NOESY spectrum, the correlations between H-3/Me-23, Me-23/H-5, H-5/H-9, H-9/Me-27, Me-27/H-18, Me-29/H-18 and Me-30 revealed that these protons were cofacial with an *α*-configuration, and the correlations between Me-25/Me-26 and Me-24 corresponded to the *β*-oriented configuration of the molecular plane. Therefore, the structure of **2** was unambiguously established as 3*β*-hydroxyurs-12-en-20,28-olide (Fig. 1), and the assignments of $^1$H and $^{13}$C NMR data (Table 1) were fully achieved.

Compound **3** was obtained as white amorphous powder. The molecular formula of $C_{30}H_{44}O_3$, with nine degrees of unsaturation, was supported by HR-ESI-MS at *m/z* 453.3363 $[M + H]^+$ (Calcd. for $C_{30}H_{45}O_3$, 453.3363). The MS/MS spectrum gave fragment ions at *m/z* 435.3257, 407.3308, 389.3202, 201.1637, and 189.1638. The IR spectrum of **3** suggested that it contained hydroxyl and carbonyl groups (3423 and 1743 $cm^{-1}$). The NMR spectral data of **3** were sim-

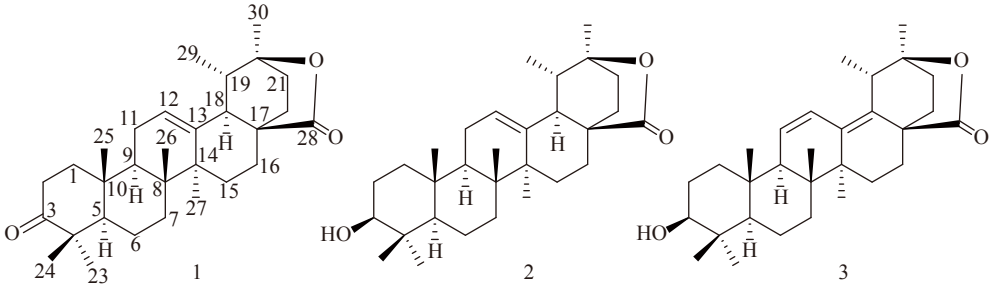

**Fig. 1 Chemical structures of compounds 1–3**

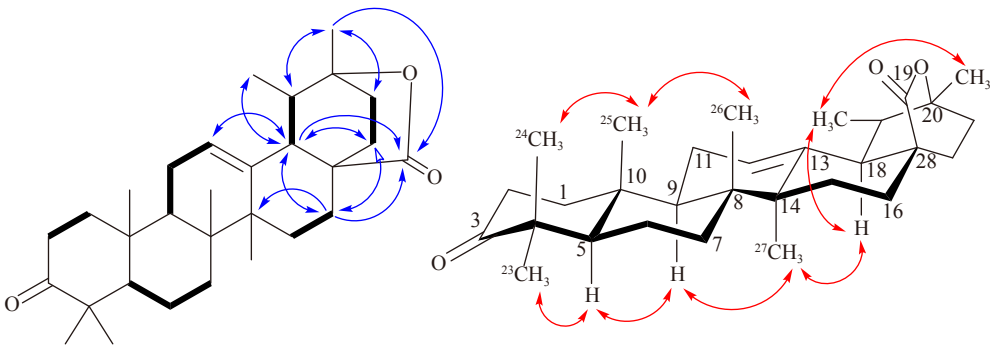

**Fig. 2 Key $^1$H-$^1$H COSY (bold lines), HMBC (blue) and NOESY (red) correlations of compound 1**

ilar to those of compound **2** except that the olefinic carbons at $\delta_C$ 121.4 and 140.6 were replaced by a set of conjugated double bond carbons at $\delta_C$ 126.1, 128.1, 134.4 and 137.4 in the $^{13}C$ NMR data (Table 1). The conjugated double bonds of **3** were confirmed by the HMBC spectrum. The long-range correlations from H-11 ($\delta_H$ 6.10) to C-8, C-9, C-10 and C-13, from H-12 ($\delta_H$ 5.73) to C-9, C-14, C-17 and C-18, from $H_3$-29 ($\delta_H$ 1.08) to C-18 and from $H_3$-27 ($\delta_H$ 0.94) to C-18 revealed that the conjugated double bonds were located at C-11 (12) and C-13 (18) in compound **3**. In combination with the NMR data (Table 1), the structure assignment of **3** was unambiguously established as 3*β*-hydroxyurs-11,13(18)-dien-20,28-olide (Fig. 1).

*Anti-inflammatory and antibacterial activities*

LPS-stimulated RAW 264.7 cells were treated with compounds 1–3 to evaluate their cell viability at concentrations of 50, 25, 10, and 5 μmol·L$^{-1}$, while a control group was simply stimulated by LPS alone. There were no obvious effects of the three compounds on cell viability determined by CCK-8 assay, which indicated that the inhibition of NO production in LPS-activated RAW264.7 cells was not induced by the cytotoxicity of the compounds. Furthermore, the three compounds were screened *in vitro* for their anti-inflammatory effects on NO production in LPS-activated RAW 264.7 cells (see Fig. 3). All three compounds exhibited significant inhibitory effects on NO production in LPS-activated RAW264.7 cells at a concentration of 50 μmol·L$^{-1}$, especially compound **1**, which exerted the strongest anti-inflammatory activity with NO production of (3.46 ± 0.24) μmol·L$^{-1}$, compared with the control (6.98 ± 0.10 μmol·L$^{-1}$). NO production of compounds **1–3** was (5.35 ± 0.23), (5.33 ± 0.07) and (5.74 ± 0.08) μmol·L$^{-1}$ at a concentration of 10 μmol·L$^{-1}$, which showed weaker NO inhibition than the positive control drug hydrocortisone (3.82 ± 0.23 μmol·L$^{-1}$).

Compounds **1–3** were evaluated for their antibacterial activities against gram-positive *Bacillus subtilis*, *Staphylococcus aureus* and methicillin-resistant *Staphylococcus aureus* (MRSA), and gram-negative *Pseudomonas aeruginosa* and *Escherichia coli*, but they were found to be inactive at a concentration of 128 μg·mL$^{-1}$.

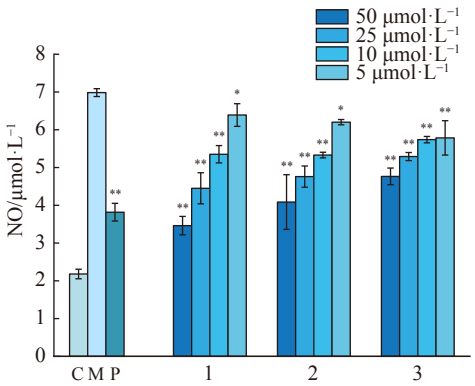


**Fig. 3 Effects of nitric oxide (NO) production in RAW246.7 cells treated with hydrocortisone and compounds 1–3. Data are expressed as mean ± SD ($n$ = 3). Statistical analysis was performed using one-way analysis of variance followed by Tukey's multiple comparison test. $^{*}P < 0.05$ and $^{**}P < 0.01$ *vs* the LPS-treated model group. C: the control group, M: the model group, P: the positive group**

## Experimental

*General experimental procedures*

Optical rotation values were measured on a JASCO P-2000 polarimeter (JASCO Inc., Tokyo, Japan). Accurate mass measurements were performed with a Thermo QE UP-LC-Orbitrap MS spectrometer (Thermo Scientific Inc., Waltham, MA, USA). IR spectra were acquired on a Thermo Nicolet IS5 FT-IR spectrophotometer (Thermo Scientific Inc., Waltham, MA, USA). 1D- and 2D-NMR spectra were acquired in $C_5D_5N$ and $CDCl_3$ with TMS as an internal standard on Bruker AV-III-500 and Bruker Avance-500 MHz spectrometers (Bruker Corporation, Billerica, MA, USA and Rheinstenten, Germany). Residual solvent shifts were referenced to $\delta_H$ 7.20, $\delta_C$ 123.44 in $C_5D_5N$, and $\delta_H$ 7.26, $\delta_C$ 77.16 in $CDCl_3$, respectively. Preparative HPLC was performed on a Waters 2535 system with a Waters 2998 dual-wavelength absorbance detector (Waters Corporation, Milford, MA, USA), using a SunFire™ $C_{18}$ preparative column (250 mm × 19 mm, 5 μm) (Waters Corporation, Milford, MA, USA). Preparative LPLC was performed with Combiflash (ISCO Companion, Lincoln NE, USA). Column chromatography was performed with silica gel (160–200 mesh, Qingdao Marine Chemical, Inc., Qingdao, China), Sephadex LH-20 and cyanopropyl silica gel (Pharmacia Biotech AB, Uppsala, Sweden).

*Plant materials*

The twigs and leaves of *Rosmarinus officinalis* (herbarium No. 20140901) were purchased from Henan Province, China, in September 2014 and authenticated by Prof. LIN Peng-Cheng at Qinghai Nationalities University. The voucher specimens were deposited at the herbarium of Beijing Key Laboratory of Bioactive Substances and Functional Foods, Beijing Union University, Beijing, China.

*Extraction and isolation*

The air-dried aboveground part of rosemary (10 kg) was powdered and extracted with 95%, 85% and 75% aqueous EtOH at room temperature for 90 min under sonication. The EtOH extract was evaporated under reduced pressures to yield a residue. The residue was dissolved in water-saturated ethyl acetate to obtain a soluble fraction (1.305 kg), and then the soluble fraction was loaded on a silica gel column eluted with a gradient of increasing methanol (0–100%, *V*/*V*) in chloroform to give eight fractions (M1–M8). Fraction M2 exhibited potential inhibitory effects against *B. subtilis* with an MIC value of 8 μg·mL$^{-1}$ and significantly inhibitory effects on NO production in LPS-activated RAW264.7 cells at a concentration of 50 μg·mL$^{-1}$.

Fraction M2 (210 g) was subjected to chromatography over silica gel using a gradient of acetone (0–100%) in petro-

leum ether, and nine fractions (M2-1 to M2-9) were obtained based on TLC analysis. Fraction M2-3 (13.0 g) was separated over a Sephadex LH-20 gel and eluted with petroleum ether/$CHCl_3$/$CH_3OH$ (5 ∶ 5 ∶ 1, *V*/*V*/*V*), to afford seven subfractions (M2-3-1 to M2-3-7). Subfraction M2-3-2 (3.2 g) was then purified by normal phase cyanopropyl silica LPLC and eluted with petroleum ether (60–90 °C)/acetone (100 ∶ 0 to 50 ∶ 1, *V*/*V*), to obtain five fractions (M2-3-2-1 to M2-3-2-5). M2-3-2-4 (90 mg) was heated and dissolved in methanol. After cooling, the white precipitate was obtained by filtration, which was further purified by preparative reversed phase HPLC and eluted with MeOH/$H_2O$ (92 ∶ 8, *V*/*V*, 18.0 mL·min$^{-1}$, monitor wavelength: 210 nm), to afford **1** (8.0 mg, $t_R$16 min). Subfraction M2-3-7 (9.0 g) was chromatographed over a Sephadex LH-20 gel and eluted with petroleum ether/$CHCl_3$/$CH_3OH$ (5 ∶ 5 ∶ 1, *V*/*V*/*V*) to afford six fractions (M2-3-7-1 to M2-3-7-6). M2-3-7-4 (2.2 g) was separated by preparative reversed-phase LPLC and eluted with a gradient of MeOH/$H_2O$ (40 ∶ 60–100 ∶ 0, *V*/*V*), to gave nine fractions (M2-3-7-4-1 to M4-7-4-9). M2-3-7-4-5 (60 mg) was further separated by preparative reversed phase HPLC, eluted with MeOH/$H_2O$ (87 ∶ 13, *V*/*V*, 18.0 mL·min$^{-1}$, monitor wavelength: 210 nm), to afford **2** (12.0 mg, $t_R$ 25 min) and **3** (6.0 mg, $t_R$ 26 min).

*Identification of new compounds*

*3-Oxours-12-en-20,28-olide (**1**)*

Amorphous white powder; $[\alpha]_D^{20}$ − 6.0 (*c* 0.05, $CHCl_3$); IR $\nu_{max}$ cm$^{-1}$: 2947, 2924, 2855, 1739, 1704, 1459, 1384, 1323, 1243, 1222, 1197; HR-ESI-MS *m*/*z* 453.3362 $[M + H]^+$ (Calcd. for $C_{30}H_{45}O_3$, 453.3363); $^1$H NMR spectral data ($C_5D_5N$, 500 MHz) and $^{13}$C NMR spectral data ($C_5D_5N$, 125 MHz): see Table 1.

*3β-Hydroxyurs-12-en-20,28-olide (**2**)*

Amorphous white powder; $[\alpha]_D^{20}$ − 30.6 (*c* 0.17, $CHCl_3$); IR $\nu_{max}$ cm$^{-1}$: 3509, 2986, 2939, 2872, 1730, 1657, 1616, 1460, 1384, 1377, 1358, 1324, 1248, 1223, 1179, 1120; HR-ESI-MS (*m*/*z*): 455.3519 $[M + H]^+$ (Calcd. for $C_{30}H_{47}O_3$, 455.3520); $^1$H NMR spectral data ($CDCl_3$, 500 MHz) and $^{13}$C NMR spectral data ($CDCl_3$, 125 MHz): see Table 1.

*3β-Hydroxyurs-11,13(18)-dien-20,28-olide (**3**)*

Amorphous white powder; $[\alpha]_D^{20}$ − 92.0 (*c* 0.35, $CHCl_3$); UV (MeOH) $\lambda_{max}$ (log ε) 259 (4.01), 198 (2.53) nm; IR $\nu_{max}$ cm$^{-1}$: 3553, 3423, 2936, 2869, 1743, 1630, 1456, 1384, 1354, 1333, 1295, 1268, 1231, 1184, 1129, 1108; HR-ESI-MS (*m*/*z*): 453.3363 $[M + H]^+$ (calcd. for $C_{30}H_{45}O_3$, 453.3363); $^1$H NMR spectral data ($CDCl_3$, 500 MHz) and $^{13}$C NMR spectral data ($CDCl_3$, 125 MHz): see Table 1.

*Anti-inflammatory activity assay*

Preliminary *in vitro* anti-inflammatory analyses of the isolated compounds on NO production in LPS-activated RAW264.7 cells were performed using established methods [15] with some modifications. The cell viability of the pure compounds and fractions was tested by CCK-8 assay. RAW264.7 cells (8 × 10$^3$/well) were seeded in 96-well plates and incubated for 24 h. The cells was treated with or without the tested compounds and fractions at given concentrations for 24 h. Then, 10 μL of CCK-8 solution was added before incubation at 37 °C for 2 h. The absorbance was measured at 450 nm by a microplate reader (Infinite M Nano, Tecan). The cell viability was determined by comparison with that of the untreated cells at 100%.

NO production was measured in the supernatants of RAW264.7 cells using a NO assay kit (Beyotime Biotech, Inc. China). The cells were cultured in 96-well (8 × 10$^3$/well) plates for 24 h and then pretreated with the tested compounds (50, 25, 10 and 5 μmol·L$^{-1}$), positive control (10 μmol·L$^{-1}$) or fractions (50 μg·mL$^{-1}$) before incubation for 1 h. Subsequently, LPS (5 μg·mL$^{-1}$) was added and the cells were cultured for another 24 h. Fifty microliters of the supernatants were taken to mix with 50 μL of Griess reagent (1% sulfanilamide, 0.1% naphthylethylenediamine dihydrochloride and 2.5% phosphoric acid) and shaken at room temperature for 5 min. The absorbance was detected at 540 nm by a microplate reader. NO production was calculated according to a sodium nitrite ($NaNO_2$) standard curve.

*Antibacterial activity assay*

The minimum inhibitory concentrations (MICs) of the fractions and isolated compounds against gram-positive *B. subtilis*, *S. aureus* and methicillin-resistant *S. aureus* (MRSA) and gram-negative *P. aeruginosa* and *E. coli* in 96-well plates were determined using the broth microdilution method according to the Clinical and Laboratory Standards Institute Guidelines, as previously described [16]. The bacteria were cultured in Mueller-Hinton broth. The fractions and pure compounds were dissolved in DMSO separately and tested at a final concentration of 128, 64, 32, 16, 8, 4, 2, 1, 0.5, 0.25, 0.125, and 0.0625 μg·mL$^{-1}$. The bacterial cultures (100 μL) of each strain were added to the wells at an inoculum density of 5 × 10$^5$ CFU·mL$^{-1}$. Samples at each concentration were added to three bacterial culture wells to ensure the repeatability of the experiment. After incubation at 37 °C for 16 h, the sample at the lowest concentration without visible bacterial growth was determined as the MIC. Rifampicin was used as a positive control.

## References


[1] Bahri S, Ben AR, Gasmi K, *et al*. Prophylactic and curative effect of rosemary leaves extract in a bleomycin model of pulmonary fibrosis [J]. *Pharm Biol*, 2017, **55**(1): 462-471.

[2] Andrade JM, Faustino C, Garcia C, *et al*. *Rosmarinus officinalis* L. : an update review of its phytochemistry and biological activity [J]. *Futur Sci OA*, 2018, **4**(2): FSO283.

[3] Yao H, Chen YF, Zhang LJ, *et al*. Carnosol inhibits cell adhesion molecules and chemokine expression by tumor necrosis factor-α in human umbilical vein endothelial cells through the nuclear factor-κB and mitogen-activated protein kinase pathways [J]. *Mol Med Rep*, 2014, **9**: 476-480.

[4] Mei YY, Huei LC, Chin CH, *et al*. Carnosic acid reduces cytokine-induced adhesion molecules expression and monocyte adhesion to endothelial cells [J]. *Eur J Nutr*, 2009, **48**(2): 101-106.

[5] Romo-Vaquero M, Larrosa M, Yánez-Gascón MJ, *et al*. A

rosemary extract enriched in carnosic acid improves circulating adipocytokines and modulates key metabolic sensors in lean Zucker rats: Critical and contrasting differences in the obese genotype [J]. *Mol Nutr Food Res*, 2014, **58**(5): 942-953.

[6] Bernardes WA, Lucarini R, Tozatti MG, *et al*. Antimicrobial activity of *Rosmarinus officinalis* against oral pathogens: relevance of carnosic acid and carnosol [J]. *Chem Biodivers*, 2010, **7**(7): 1835-1840.

[7] Moreno S, Scheyer T, Romano CS, *et al*. Antioxidant and antimicrobial activities of rosemary extracts linked to their polyphenol composition [J]. *Free Radic Res*, 2006, **40**(2): 223-231.

[8] Mushtaq W, Naim A, Naeem S. *In vitro* anti-bacterial activity of *rosmarinus officinalis* L. and *murraya koenigii* L. against multi-drug resistant staphylococcus species [J]. *Int J Biol Biotechnol*, 2019, **16**(4): 1005-1010.

[9] Beninca JP, Dalmarco JB, Pizzolatti MG, *et al*. Analysis of the anti-inflammatory properties of *Rosmarinus officinalis* L. in mice [J]. *Food Chem*, 2011, **124**(2): 468-475.

[10] Arranz E, Jaime L, García-Risco MR, *et al*. Anti-inflammatory activity of rosemary extracts obtained by supercritical carbon dioxide enriched in carnosic acid and carnosol [J]. *Int J Food Sci Tech*, 2015, **50**(3): 674-681.

[11] Diniz-Silva HT, Batista dSJ, Guedes Jessica dS, *et al*. A synergistic mixture of *Origanum vulgare* L. and *Rosmarinus officinalis* L. essential oils to preserve overall quality and control Escherichia coli O157: H7 in fresh cheese during storage [J]. *LWT - Food Sci Tech*, 2019, **112**: 107781.

[12] Hicham B, Zahra B. Investigation of antibacterial and antioxidant activities of rosemary essential oil from Algeria [J]. *Res J Pharm Biol Chem Sci*, 2017, **8**(3): 1425-1434.

[13] Matsuo Y, Watanabe K, Mimaki Y. Triterpene glycosides from the underground parts of *Caulophyllum thalictroides* [J]. *J Nat Prod*, 2009, **72**(6): 1155.

[14] Li LL, Sun Z, Shang XY, *et al*. Triterpene compounds from *Cirsium setosum* [J]. *China J Chin Mater Med*, 2012, **37**(7): 951-955.

[15] Zhao JH, Shen T, Yang X, *et al*. Sesquiterpenoids from *Farfugium japonicum* and their inhibitory activity on NO production in RAW264.7 cells [J]. *Arch Pharm Res*, 2012, **35**(7): 1153-1158.

[16] Li J, Chen MH, Hao XM, *et al*. Structural revision and absolute configuration of burnettramic acid A [J]. *Org Lett*, 2020, **22**(1): 98-101.

**Cite this article as:** ZHONG Xiang-Jian, ZHOU Na, WANG Xin, LI Jin-Jie, MA Hui, JIAO Yue, XU Jia-Hui, LIN Peng-Cheng, SHANG Xiao-Ya. Three new ursane-type triterpenoids from *Rosmarinus officinalis* and their biological activities [J]. *Chin J Nat Med*, 2022, **20**(2): 155-160.